Ab Initio Study of the Structures and Vibrational Spectra of Some Diamine Radical Cations

A. M. Brouwer

Amsterdam Institute of Molecular Studies, University of Amsterdam, Laboratory of Organic Chemistry, Nieuwe Achtergracht 129, NL-1018 WS Amsterdam, The Netherlands

Received: January 8, 1997; In Final Form: February 26, 1997[⊗]

Two different types of radical cations have been studied by means of density functional theory (BLYP) and mixed Hartree−Fock/DFT (B3LYP) calculations. For the description of the structure and the vibrational frequencies of aromatic amine radical cations the latter is the best practical method, as illustrated for the case of *N*,*N*,*N*′,*N*′-tetramethyl-*p*-phenylenediamine. For the through-bond coupled radical cations of piperazine derivatives, HF calculations give completely incorrect results due to the tendency to localize the positive charge on one of the amino groups. Post-HF corrections are troublesome. The DFT calculations do not suffer from this problem, which gives them a unique advantage over HF methods in this case.

1. Introduction

Density functional theory (DFT) has made a remarkable impact on the practice of molecular quantum chemistry[1,2] in recent years following the development of nonlocal gradient-corrected functionals[1,3−6] and the widespread availability of various DFT methods in standard easy-to-use software packages.[7,8]

DFT calculations have shown their superiority to Hartree−Fock (HF) calculations in many areas, such as vibrational force fields and IR intensities of closed-shell molecules[9] and various properties of radical ions.[10,11] Because orbital relaxation and correlation effects can apparently be balanced properly, it has been possible to calculate ionization potentials[12] and electron affinities[13,14] by directly comparing the energies of the closed-shell ground-state molecule and the corresponding radical ion. Recent papers have shown that the vibrational force fields of aromatic radicals such as the phenoxyl radical[15] and the radical cations of aniline and *N*,*N*-dimethylaniline[16] are described remarkably well. In this area simple HF methods perform very badly, and CASSCF calculations are at least required to obtain acceptable vibrational force fields.[17,18]

In experimental studies we are currently engaged in the investigation of two types of radical cations by means of optical absorption and resonance Raman spectroscopy, viz. aniline derivatives[16] and piperazines.[19] The interpretation of the spectra obtained requires the support of high-level quantum-chemical calculations. In this paper we evaluate the performance of DFT and HF/DFT methods, in particular BLYP[3,4] and B3LYP,[6] for structures and vibrational force fields of some representative radical cations. An ideal test case is the radical cation of *N*,*N*,*N*′,*N*′-tetramethyl-*p*-phenylenediamine (TMPD), for which experimental vibrational spectra[20] and crystal structure data[21] are available. For some (substituted) piperazine radical cations the optical absorption spectra and resonance Raman spectra clearly indicate a charge-delocalized structure,[19] while other piperazine radical cations show a localization of charge and spin on one of the amino groups.[22] In view of the relatively large size of the molecules of interest (see Figure 1), we have chosen to use the 6-31G* basis set. Although this is of modest size, and not at all optimized for use with the DFT formalism, the combination B3LYP/6-31G* has been demonstrated to be very cost-effective for the calculation of vibrational force fields of neutral closed-shell molecules.[23,24] As we shall show, this also holds true for radical cations, although slightly different frequency scale factors are needed for the UB(3)LYP calculations. All calculations were carried out with the Gaussian series of programs.[7,8]

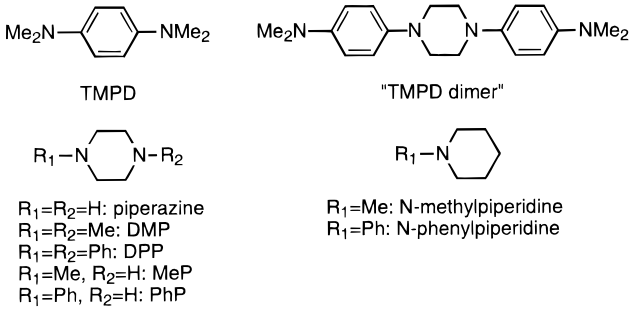

Figure 1. Compounds discussed and names or abbreviations used for them. Radical cations will be denoted simply by adding a + after the code; the radical dot is omitted.

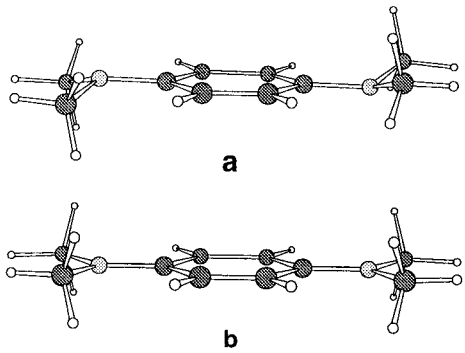

Figure 2. Computed molecular structures (B3LYP/6-31G*) of TMPD (a) and $TMPD^+$ (b).

2. TMPD: Molecular Structure of the Radical Cation

The computed lowest energy structure (Figure 2) of TMPD belongs to the C_{2h} point group. For the neutral molecule, the potential energy surface for twisting and pyramidalizing the amino groups is rather shallow. The lowest energy minimum is shown in Figure 2. The crystal structure of TMPD was not resolved to very high precision, and the result does not reflect the full symmetry of the free molecule. The bond lengths listed in Table 1 are averaged over the symmetry equivalent bonds.

[⊗] Abstract published in *Advance ACS Abstracts,* April 15, 1997.

S1089-5639(97)00142-4 CCC: $14.00

TABLE 1: Bond Lengths (Å) of TMPD and TMPD^{+a}

	TMPD		TMPD$^+$			
bond	exp[b]	B3LYP	exp[c]	UHF	UBLYP	UB3LYP
C_1-N	1.41 (1.43)	1.405	1.355	1.334	1.372	1.357
N−Me	1.44 (1.49)	1.452	1.452	1.464	1.480	1.468
C_1-C_2	1.40 (1.38)	1.408	1.415	1.429	1.438	1.430
C_2-C_3	1.39 (1.38)	1.392	1.362	1.354	1.383	1.371

[a] Computed values from this work, using the 6-31G* basis set. [b] Reference 54 (CSD[55] refcode TMPPDA), symmetry-averaged; values in parentheses for TMPD/tetracyanobenzene complex, ref 56 (CSD refcode TPDTCB), symmetry averaged. [c] TMPD perchlorate, ref 21 (CSD refcode TMPDPC).

For comparison, data for the TMPD/tetracyanobenzene complex are included.

The B3LYP structure for the neutral TMPD is in excellent agreement with the X-ray data. The sum of the bond angles around the nitrogen atoms is found to be 352°, intermediate between the values expected for ideal tetrahedral (328.4°) and planar (360°) geometries.

The crystal structure of TMPD perchlorate has been studied in detail by de Boer and Vos.[21,25] The radical cation also has C_{2h} symmetry, although the molecular framework is essentially planar (D_{2h}). In Table 1 the calculated bond lengths at three levels of theory are compared with the experimental data. It can be seen that a good agreement is found for all three levels, the BLYP bond lengths being somewhat too long, a systematic deviation also noted for neutral molecules.[5] Although UHF calculations do not generally yield good vibrational force fields for aromatic radicals,[15−17,26] the computed structure is not too bad. We note that the spin contamination is much less severe in this case ($\langle S^2\rangle = 0.82$) than in for example *N*,*N*-dimethylaniline radical cation ($\langle S^2\rangle = 1.29$).[16]

TMPD and related compounds have been extensively applied in studies of electron transfer processes. The change in molecular structure upon addition or removal of an electron and the energy associated with this geometry change are important factors in determining the rate of an electron transfer reaction.[27] The internal reorganization energy, λ_i, involved in the self-exchange process (eq 1) has been estimated in different ways.

$$\mathrm{TMPD} + \mathrm{TMPD}^+ \rightleftarrows \mathrm{TMPD}^+ + \mathrm{TMPD} \qquad (1)$$

Grampp and Jaenicke[28] used the experimentally known bond length differences between TMPD and TMPD$^+$ and estimated force constants for bond stretching. Nelsen,[29] and Rauhut and Clark[30] simply evaluated λ_i according to eq 2 using AM1 calculations of the energies of the radical cation and the neutral molecule at their own equilibrium geometries ($E(c^+)$ and $E(n^0)$, respectively) and at the geometry of the other species ($E(n^+)$ and $E(c^0)$ denoting the energy of the cation at the neutral geometry and the energy of the neutral at the geometry of the cation, respectively).[31]

$$\lambda_i = E(n^+) - E(c^+) + E(c^0) - E(n^0) \qquad (2)$$

Experimental rate data of the TMPD/TMPD$^+$ self-exchange, determined using EPR experiments at 293 K,[32] were initially interpreted assuming an adiabatic electron transfer process and yielded a small internal reorganization energy of $\lambda_i = 5.1$ kcal/mol. Later,[28] slightly higher values were estimated and used in a different interpretation of more extensive sets of experimental data. Spectroscopic data for the radical cation of the "TMPD dimer" 1,4-bis(4-(dimethylamino)phenyl)piperazine (Figure 1) show that for this system $\lambda_i \approx 21$ kcal/mol.[29] The latter value is in agreement with semiempirical AM1 quantum-chemical calculations, which for TMPD/TMPD$^+$ gave values of λ_i of 18.7−27.7 kcal/mol.[29,30] Since the DFT and HF/DFT methods appear to give simultaneously good structures and force constants (see below) for the neutral molecule and the radical cation, they should also be able to provide good estimates of λ_i. The reorganization energies calculated with Nelsen's approach (eq 2) are found to be 10.0 kcal/mol with the BLYP method and 12.2 kcal/mol using B3LYP. The contribution of geometry relaxation in the cation is larger than that of the neutral molecule. The values obtained here are in between the high values from AM1 calculations and the low values estimated by Grampp and Jaenicke. Nelsen's value for the "TMPD dimer" is higher because of differences in geometry due to the ring structure and might also be biased by an underestimation of the solvent reorganization energy λ_{out}.

It should be kept in mind that there is not necessarily a simple relationship between the internal energy calculated here and the free energy quantities in Marcus theory.[33] The reorganization energy depends strongly on the geometry chosen for the neutral molecule.[29−31] The energy surface is quite shallow, and low-energy configurations are accessible which may have a much smaller reorganization energy than the global minimum structure. Experimentally, the internal reorganization energy is usually hard to determine. Therefore, the ability to compute the internal energy contribution to λ_i may still be helpful for the interpretation of electron transfer kinetics.[34,35]

3. TMPD Radical Cation: Vibrational Force Field

The radical cation of TMPD was among the first aromatic radicals to be studied by means of resonance Raman spectroscopy in solution.[20,36−38] For the parent phenylenediamine radical cation Chipman et al.[39] used UHF calculations to interpret the vibrational spectra, but in view of the failure of this approach in other cases[15,16] more generally reliable methods are needed. Results of experiment and computation (BLYP/6-31G* and B3LYP/6-31G*) are compared in Table 2. Because experimental data only cover the range below 1700 cm^{-1}, the C−H stretching region was not considered. Frequencies were scaled linearly to minimize the root-mean-square (rms) difference between calculated and observed values (35 bands of four isotopomers). Optimal scaling factors were found to be 0.982 for B3LYP and 1.020 for BLYP. These scale factors are slightly higher than the recommended values of Scott and Radom (BLYP, 0.9945; B3LYP, 0.9614)[23] and of Rauhut and Pulay (BLYP, 0.995; B3LYP, 0.963),[9] which were derived for neutral closed-shell systems. The agreement for the scaled B3LYP frequencies was slightly better, rms values of the difference between experiment and theory being 14 and 16 cm^{-1}, respectively. The largest deviation was 32 cm^{-1} for B3LYP and 41 cm^{-1} for BLYP.

It is clear that both calculations allow a straightforward assignment of the resonance Raman spectrum. Further improvement can, of course, be achieved by scaling individual force constants or groups of force constants, but this seems hardly worthwhile. We shall briefly discuss the assignment of the Raman bands on the basis of the B3LYP frequencies and normal modes. Poizat et al. assigned the spectrum of TMPD$^+$ and three deuteriated isotopomers using an empirical approach. A problem with this approach is that the effect of isotopic substitution alters the frequencies as well as the composition of many modes. Our calculations show that some of the assignments of Poizat et al. were not correct. For the parent isotopomer the 17 totally symmetric normal modes in the spectral region of interest are graphically presented in Figure 3.

TABLE 2: Frequencies (cm^{-1}) of Totally Symmetric Vibrations of the TMPD Radical Cation in the Range below 1700 cm^{-1}, Observed Experimentally,[20] and Calculated at the UBLYP/6-31G* and UB3LYP/6-31G* Levels[a]

d_0			d_4			d_{12}			d_{16}			
B3LYP	BLYP	exp	B3LYP	BLYP	exp	B3LYP	BLYP	exp	B3LYP	BLYP	exp	approx description
113	105		113	105		83	77		83	77		Me rotation
192	193		187	189		174	175		170	171		out-of-plane ring bend
306	308	330	306	308	338	279	281	300	279	281	295	in-plane ring bend
392	393		380	382		376	378		363	365		*N*-pyramidalization
533	538	517	530	535	520	476	481	460	474	479	457	CNC bend
722	725		645	646		720	723		644	644		4
767	768	770	746	748	750	736	738	743	720	723	725	6a
926	926	932	930	930	948	827	831	828	816	820	820	1
952	946		799	796		951	945		798	795		5
1130	1137		1130	1137		897	900		897	901		Me wag
1175	1180	1175	1176	1182	1175	1019	1026	1025	1020	1026	1025	Me rock
1235	1247	1228	879	887	888	1234	1246	1222	886	896	890	9a
1437	1421	1420	1433	1416	1430	1448	1424	1465	1444	1419	1458	ν(N-ring)
1482	1496		1481	1495		1142	1147		1141	1147	1157	Me deformation
1498	1514	1512	1498	1514	1515	1080	1092		1079	1092		Me deformation
1533	1546		1533	1545		1086	1099		1087	1100		Me deformation
1655	1647	1632	1622	1613	1610	1654	1646	1632	1621	1612	1607	8a

[a] Scaling factor 0.982 for B3LYP, 1.02 for BLYP.

Experimentally, for the parent isotopomer nine bands were observed that were attributed to fundamentals. The band at 1632 cm^{-1} clearly corresponds to the typical 8a vibration, but the observed fundamental at 1512 cm^{-1} is due to a methyl deformation mode, rather than to N-ring stretching. This latter mode is found at 1420 cm^{-1}, not at 1512 cm^{-1}. The frequency of ν(N-ring) is not strongly affected by deuteriation of the ring, but it increases considerably upon deuteriation of the methyl groups. The ν(N-ring) bands at 1465 cm^{-1} in the d_{12} isotopomer and at 1458 cm^{-1} in d_{16} have been correctly assigned by Poizat et al.

The observed band at 1228 cm^{-1} is mode 9a; 1175 cm^{-1} corresponds to methyl rocking, as correctly inferred by Poizat. The weak band at 932 cm^{-1} corresponds to ring breathing (mode 1); the one at 770 cm^{-1} is more like 6a. The bands observed at low frequencies, 517 and 330 cm^{-1}, are due to bending modes localized mostly on the dimethylamino groups and the benzene ring, respectively.

The results presented here show that the B3LYP method is somewhat better in predicting the vibrational frequencies of the TMPD radical cation than the BLYP approach. In particular, the complex response of the the ν(N-ring) mode to deuteriation is better reproduced by the UB3LYP calculations (Table 2).

4. Piperazine Radical Cations

Radical cations of simple amines are rather unstable species, but we have found that their optical absorption and resonance Raman spectra can be studied conveniently when the radical ions are generated via pulsed laser-induced oxidation, allowing their detection as transient species which decay mainly by charge recombination rather than undergoing decomposition reactions.[16,19] An interesting aspect of the radical cations of bifunctional amines such as piperazines is the issue of charge localization on one amino group vs charge delocalization over the two centers. We have shown that in the case of the symmetric *N*,*N*-dimethylpiperazine (DMP) the radical cation has a delocalized nature.[19] In asymmetric systems charge localization should occur when the difference in the ionization potentials of the two amino groups is large enough relative to the electronic interaction between the amino groups. Recent experiments have shown that the optical absorption band characteristic of the charge-delocalized structure is also present in the spectra of the radical cations of *N*-phenylpiperazine (PhP), *N*-methylpiperazine[40] (MeP), and *N*,*N*-diphenylpiperazine (DPP).[22] This band is found at 600 nm for DMP^+, 550 nm for MeP^+, 700 nm for PhP^+, and >900 nm for DPP^+. The relative positions of the absorption bands can be rationalized qualitatively by a simple model, originally described for dimer cations,[41] which predicts that a red shift of the band should occur as a result of weaker coupling between the components and a blue shift as a consequence of asymmetry. In the phenyl systems weaker coupling is likely to result from delocalization of the excess positive charge and spin into the aromatic ring, decreasing the spin density on the nitrogen atom. A noteworthy feature is the absence of the characteristic aniline radical cation absorption band, typically found near 470 nm, in the spectra of PhP^+ and DPP^+. When a 4-methoxy group is introduced into the aniline moiety, however, the typical localized aniline absorption is present again, even if the neutral molecule is symmetric.[22] For the radical cation of the "TMPD dimer" 1,4-bis(4-(dimethylamino)phenyl)piperazine compelling experimental evidence has been presented for a charge-localized, symmetry-broken structure.[29] Apparently, in these cases the electronic coupling is too small to maintain a delocalized structure, which presumably has a higher reorganization energy than the symmetry-broken geometry.

We have previously reported that HF calculations incorrectly predict DMP^+ to be asymmetric, charge-localized, while MP2 correlation correction is large and favors the symmetric charge-delocalized structure. The most stable geometry of DMP^+ (UMP2/6-31G*) was found to be a symmetric chair conformation, in which through-bond coupling is optimized by placing the methyl groups in a pseudoaxial orientation.[19] Boat conformers which would optimize through-space N−N interaction were ruled out on the basis of the computed relative energies. Moreover, the vibrational frequencies were found to be in much better agreement with the computed frequencies for the chair form.

A serious problem with the HF calculations in this case is that the wave functions are unstable with respect to breaking of the spatial symmetry.[42,43] In spite of this, rather good vibrational frequencies (when scaled appropriately) were predicted for the totally symmetric modes.

For asymmetric systems, e.g. MeP^+, different charge-localized forms could be generated in UHF calculations by starting from a properly chosen initial geometry. This result, which is in conflict with experimental data, is attributed to the intrinsic tendency of HF calculations toward charge localization. At-

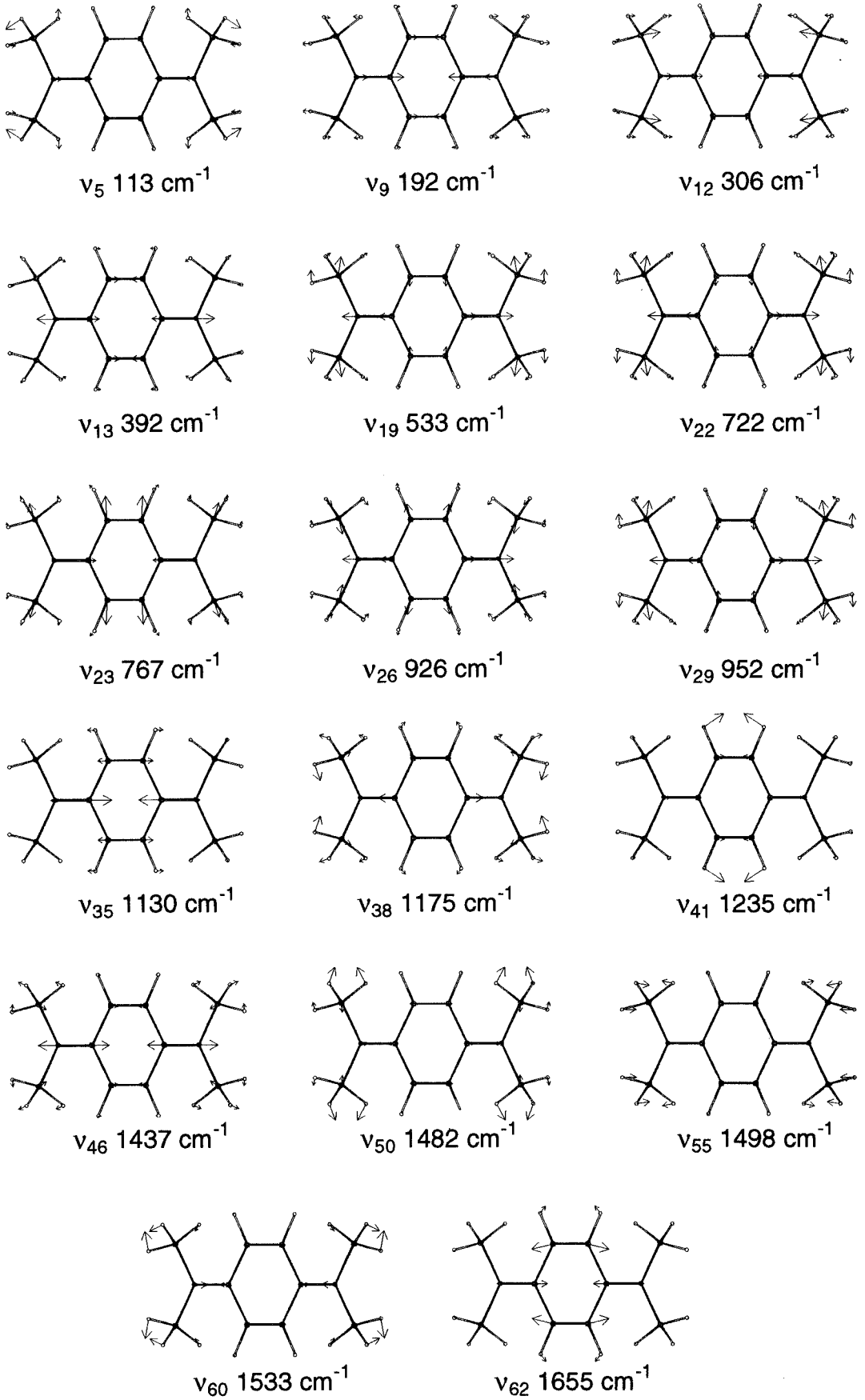

Figure 3. Totally symmetric normal modes of vibration of $TMPD^+$ (UB3LYP/6-31G*).

tempts to perform UMP2 geometry optimizations on MeP^+ or on DMP^+ and piperazine$^+$ without a constraint enforcing 2-fold symmetry led to serious convergence problems. Clearly, it would be attractive to take dynamical electron correlation into account from the start, rather than trying to add it afterward as a perturbation. Thus, it is of interest to see how well DFT methods perform for these problems.

For all piperazine radical cations studied, UBLYP and

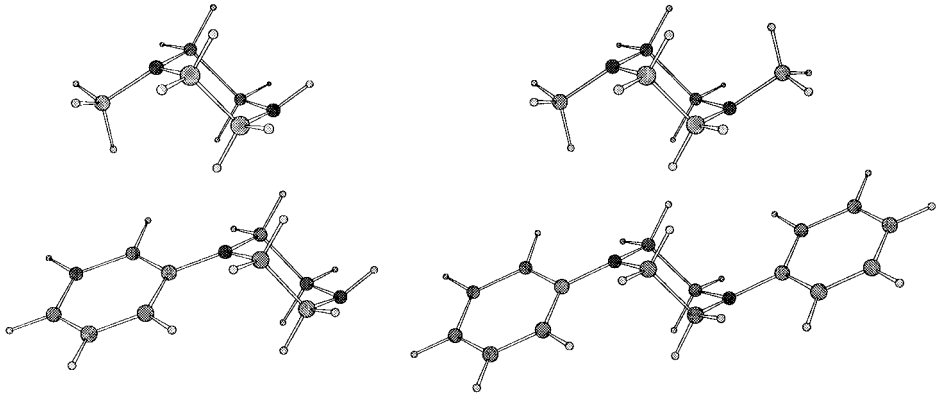

Figure 4. UB3LYP/6-31G* optimized molecular structures of MeP^+ (C_s), DMP^+ (C_{2h}), PhP^+(C_1), and DPP^+ (C_i).

TABLE 3: Selected Geometric Parameters of Optimized Structures of DMP and DMP^+ (6-31G* Basis Set)[a]

	DMP			DMP^+		
feature	HF	BLYP	B3LYP	HF	BLYP	B3LYP
r_{CC} (Å)	1.5207	1.5395	1.5274	1.6182	1.6174	1.6075
$a_{C_2-N-C_6}$ (deg)	110.78	110.09	110.29	114.43	113.80	113.96
a_{C_2-N-Me} (deg)	112.30	111.94	112.00	118.87	118.85	118.77

[a] r_{CC} is the C2−C3 (C5−C6) bond length.

TABLE 4: Characteristic Features of the Optimized Geometries of MeP and PhP (NH−ax as Well as NH−eq) and Their Radical Cations[a]

		neutral			cation			
compd	method	r_{CC}	ΣN1	ΣN2	r_{CC}	ΣN1	ΣN2	r(C1−N)
MeP	BLYP	1.540	334.2	329.2	1.624	352.7	348.5	
	B3LYP	1.528	334.6	330.5	1.612	352.9	348.8	
DMP	BLYP	1.540	334.0	334.0	1.617	351.5	351.1	
	B3LYP	1.528	334.3	334.3	1.608	351.5	351.1	
N-phenylpiperidine	B3LYP	1.533	346.7		1.543	359.8		1.365
PhP N−H ax	BLYP				1.595	358.1	354.1	1.405
	B3LYP				1.579	357.9	343.2	1.388
PhP N−H eq	B3LYP	1.529	346.7	330.4	1.549	359.4	341.4	1.371
DPP	BLYP				1.584	356.7	356.7	1.414
	B3LYP				1.575	356.0	356.0	1.404

[a] r_{CC} is the length of the C2−C3 and C5−C6 bonds (averaged in asymmetric molecules). ΣN is the sum of the bond angles around the nitrogen atoms. r(C1−N) (Å) refers to the C−N bond length of the arylamine part.

UB3LYP geometry optimizations yielded a single optimized geometry (Figure 4), with only one exception (see below). For piperazine$^+$, DMP^+, and DPP^+ asymmetric starting geometries readily converged to the symmetric structure.

Geometric parameters of DMP^+ obtained with the different methods are very similar, as shown in Table 3.

When the DMP^+ geometry is optimized starting from the structure of the neutral molecule, in which the methyl groups occupy the usual equatorial positions, a spontaneous nitrogen inversion occurs which puts both N substituents in a pseudoaxial orientation. This phenomenon and the rather long C2−C3 and C5−C6 bonds are typical manifestations of through-bond 1−4 interaction.[44−46]

We have previously published the vibrational frequencies of totally symmetric modes of DMP^+ observed experimentally and calculated using UHF theory.[19] For eight observed fundamentals the optimal UHF scaling factor was 0.909, the rms deviation of observed and computed frequencies was 21 cm^{-1}, and the largest deviation was 38 cm^{-1}. The UBLYP/6-31G* frequencies required scaling by 1.016 and gave essentially the same rms (22 cm^{-1}) and largest deviation (37 cm^{-1}). UB3LYP was somewhat better, with a scale factor of 0.982, rms deviation of 19 cm^{-1}, and largest deviation of 35 cm^{-1}. It is remarkable that the optimal scale factors derived for UBLYP and UB3LYP for this particular case are the same as for the chemically rather different $TMPD^+$.

For MeP^+ as well as for PhP^+ structures were found with the same characteristic structural features as noted for DMP^+. With the B3LYP method MeP^+ showed only one energy minimum, but for PhP^+ we could locate structures with the N−H group axially or equatorially positioned, the former being 2.13 kcal/mol lower in energy. Charge-localized structures did not correspond with stable energy minima according to the DFT calculations. Geometric parameters obtained for asymmetric piperazines and their radical cations are given in Table 4. Data on DMP and DPP and on *N*-phenylpiperidine[40] are included for comparison.

Experimental data on the molecular structures of these radical cations are not available. A very strong indication that they are all charge-delocalized follows from the optical absorption spectra, as mentioned above. Clearly, the geometric parameters correlate with the extent of charge (spin) delocalization onto the aromatic rings in the phenyl derivatives (see below, Table 5). For PhP^+ the BLYP method predicts strong delocalization, resulting in a longer CC bond, a longer CN bond between the phenyl and piperazine rings, and a partial flattening of both amino groups. The B3LYP method on the other hand apparently tends to localize the "hole" more on the phenyl ring, especially in the N−H equatorial conformation in which the lone pair on N-4 is not in the optimal orientation for interaction.

In the asymmetric systems it is of interest to have a measure of the electronic asymmetry which can be compared with

TABLE 5: Computed Spin Densities on the N Atoms in Radical Cations

compd	method	ρ(N1)	ρ(N4)
MeP	BLYP	0.42	0.31
	B3LYP	0.46	0.30
DMP	BLYP	0.37	0.37
	B3LYP	0.38	0.38
N-phenylpiperidine	BLYP	0.44	
	B3LYP	0.48	
PhP N−H ax	BLYP	0.34	0.21
	B3LYP	0.41	0.16
PhP N−H eq	B3LYP	0.45	0.05
DPP	BLYP	0.24	0.24
	B3LYP	0.27	0.27

TABLE 6: B3LYP/6-31G* Calculated Vibrational Frequencies (cm^{-1}) (Scaled × 0.982) of the 8a Vibration in Aromatic Amines and Their Radical Cations

compd	neutral	radical cation
N-phenylpiperidine	1634	1593
PhP N−H ax	1634	1598
PhP N−H eq	1634	1594
DPP	*a*	1610 (a_g) 1605 (b_u)

[a] Not calculated.

experimental data. One possibility is to look at the spin densities on the nitrogen atoms, which should be related to hyperfine splittings in EPR spectra. The computed results are given in Table 5. In particular, for PhP^+ there is a distinct difference between the spin densities calculated with the BLYP and B3LYP methods: the former tends to delocalize the charge and spin more than the latter. Unfortunately, experimental data are not available.

In relation to our experimental work in progress the vibrational frequencies of the radical cations are of interest. Some of them may serve as a measure of the electron deficiency of the aromatic ring. For example, the frequency of the characteristic 8a vibration was shown experimentally to shift by −37 cm^{-1} upon ionization of *N*,*N*-dimethylaniline.[47] In Table 6 the computed frequencies for the 8a vibration in the two conformers of PhP^+ are compared with those in N-phenylpiperidine and DPP.

It can be seen that the 8a vibration has the same frequency in the neutral molecules, as expected. In PhP^+ with the N−H equatorial the charge delocalization is computed to be small, and the 8a vibration is predicted to be almost at the same frequency as in *N*-phenylpiperidine$^+$. When the N−H is axial, however, the hole is more delocalized, and a small but probably measurable increase in the 8a frequency is calculated. When the hole is shared by the two aniline moieties in DPP^+, the frequency is calculated to be in between that of the neutrals and *N*-phenylpiperidine$^+$. Due to technical limitations, we have not yet been able to obtain the resonance Raman spectra of PhP^+ and DPP^+, but we hope to do this in the near future.

5. Ionization Energies

The B3LYP combination of functionals was developed for thermochemical purposes.[6] If it performs equally well for neutral molecules and radical cations, it should allow a good prediction of ionization energies. In Table 7 we list some energetic quantities that can be evaluated simply from energies obtained for neutral and radical cation at the two equilibrium geometries. The vertical ionization potential (IP_v) is $E(n^+) - E(n^0)$; the adiabatic (relaxed) IP_a is $E(c^+) - E(n^0)$. For comparison of oxidation potentials, which are typically measured in a polar solvent such as acetonitrile ($\epsilon = 37$), we computed the solvation energies of the neutral molecule and the radical cations (using isolated molecule geometries) and subtracted the difference from IP_a to give IP_s. We used the isodensity polarized continuum method (IPCM),[48] or its self-consistent variation (SCIPCM), which appears to be among the most promising approaches within the dielectric continuum approxiation. Nothing is known about the accuracy or reliability of these methods when applied to radical cations, so it is of interest to see what the results are.

It is clear that the ionization potentials of all three amines are underestimated by both DFT calculations, the disagreement for BLYP being greater than for B3LYP. The calculations incorrectly predict that DMP would have a lower IP_v than *N*-methylpiperidine. The computed relaxation energy ($IP_v - IP_a$) of $TMPD^+$ is somewhat smaller than the experimental value. The relaxation energy for *N*-methylpiperidine, on the other hand, is overestimated, although the B3LYP value of 0.73 eV is not too far from the experimental 0.57 eV. When comparing results from computation and experiment, both should be approached critically, but serious errors in the experimental IP_v values seem highly unlikely.

The "traditional" Koopmans IP's, the negative energies of the highest occupied MOs, are 9.37 eV for *N*-methylpiperidine and 9.38 eV for DMP. Both are too high, but the small difference is in better agreement with experiment than the DFT results.

Unfortunately, we cannot compare the solvation energies of all three compounds with the same method because the IPCM calculation failed to converge for $TMPD^+$ and SCIPCM failed for *N*-methylpiperidine$^+$. $TMPD^+$ is a more extended radical cation, and its SCIPCM solvation energy is smaller than that of DMP^+: 44.1 vs 50.3 kcal/mol. Translating the solvation energies into ion radii using the Born equation, we find r_{ion} = 3.66 Å for $TMPD^+$ and r_{ion} = 3.21 Å for DMP^+. These ion radii are reasonable, although somewhat smaller than the values typically used in estimating solvation energies of radical ions in the electron transfer field. The IPCM solvation energy calculated for the delocalized DMP^+ (48.1 kcal/mol) is smaller than that of *N*-methylpiperidine$^+$ (50.2 kcal/mol), but the difference is not very large. The computational prediction is

TABLE 7: Predicted Observables Related to Energy Differences (eV) at Different Geometries of Neutral Molecules and Corresponding Radical Cations[a]

	TMPD			DMP			*N*-methylpiperidine		
	BLYP	B3LYP	exp	BLYP	B3LYP	exp	BLYP	B3LYP	exp
IP_v	5.62	5.99	6.75[b]	7.17	7.70	8.77[c] 8.41[d]	7.70	7.97	8.37[e]
IP_a	5.34	5.65	6.20[b]	6.35	6.77		6.95	7.24	7.80[e]
IP_s/E_{ox}		3.87[f]	0.16		4.66[f] 4.79[g]	0.89		5.15[g]	0.80
λ_i	0.43	0.53		1.45	1.60		1.23	1.22	

[a] IP_v is the vertical ionization potential calculated as the energy difference between the radical cation and the neutral molecule; IP_a is the adiabatic IP. IP_s denotes IP_a minus the computed solvation energy difference (SCIPCM or IPCM) of radical cation and neutral molecule; λ_i is the internal reorganization energy for the self-exchange process (eq 2). E_{ox} is the experimental one-electron oxidation potential (in acetonitrile, vs SCE) in the case of TMPD, the anodic peak potential for the other two compounds (in methanol/water, vs SCE). [b] Reference 57. [c] Reference 58. [d] Reference 59. [e] Reference 60. [f] SCIPCM. [g] IPCM.

that DMP should have a higher oxidation potential by 0.79 V than TMPD, and *N*-methylpiperidine should be higher by another 0.36 V. Electrochemical oxidation in polar solution is irreversible for the latter two compounds,[49] so that true oxidation potentials are not known. The anodic peak potentials (0.80 and 0.89 V vs SCE for *N*-methylpiperidine and DMP, respectively) can be taken as lower limits.

Several studies have been described in which piperazine units were incorporated in intramolecular electron donor−acceptor assemblies. The charge-separated excited states in such molecules typically show a distinctly red-shifted emission compared with analogous systems containing monoamines (piperidines).[50−52] This is consistent with a lower oxidation potential and with a larger reorganization energy. Aliphatic and aromatic amines form fluorescent exciplexes with aromatic chromophores such as anthracene and pyrene. Piperazines also quench the fluorescence of such electron acceptors, but emissive exciplexes have not been observed.[53] It is likely that the large reorganization energy is responsible for a relatively rapid nonradiative decay in this case.[52]

6. Concluding Remarks

From a practical point of view, HF calculations can be used to calculate vibrational force fields for neutral ground-state molecules with moderate but often sufficient accuracy. DFT methods are more accurate, but more time-consuming, depending on the software used. For radical cations, on the other hand, HF methods are insufficient. For the σ-coupled delocalized radical cations exemplified by the piperazine derivatives, the tendency of HF to localize charge leads to completely incorrect results, which cannot be easily remedied by post-HF correlation correction. In spite of these problems, UHF leads to reasonable results for the structure and force field for totally symmetric vibrations when symmetry is present and can be imposed. Of the DFT methods studied here, B3LYP performs somewhat better than BLYP, but it is also slightly more expensive to use.

Preliminary uniform frequency scale factors were derived for the UBLYP/6-31G* and UB3LYP/6-31G* methods applied to radical cations of the two different types studied here. The values are 1.020 and 0.982, respectively. A number of radical cations are currently being studied experimentally, which will allow us to obtain statistically better scale factors in the near future.

There are two important practical factors that determine the choice of a computational approach, viz., availability of a software implementation and experience with the method documented in the literature. Our choice of B(3)LYP and a standard Gaussian basis set has been determined by these factors. The encouraging results obtained may further contribute to the popularity of this particular method. Nevertheless, it should be realized that other choices of DFT and of basis set could have led to better results.

One aspect for which the calculations discussed here are not entirely satisfactory are the ionization energies. These are underestimated, by BLYP more than by B3LYP, but also the relative values do not agree with experiment.

The BLYP method tends to predict stronger charge delocalization than B3LYP in through-bond coupled piperazine radical cations. The asymmetric piperazine radical cations may provide a very sensitive test for this feature. For example, the optical absorption spectrum of PhP^+ is indicative of a fully delocalized radical cation, but the results of the B3LYP calculations do not completely agree with this. Further experiments are clearly needed to confirm the delocalized nature of PhP^+.

Acknowledgment. This research was sponsored by the Stichting Nationale Computer Faciliteiten (National Computing Facilities Foundation, NCF) for the use of supercomputer facilities and supported (in part) by the Netherlands Foundation for Chemical Research (SON), with financial support from the Nederlandse Organisatie voor Wetenschappelijk Onderzoek (Netherlands Organization for Scientific Research, NWO). I thank Wybren-Jan Buma for critically reading the manuscript.

References and Notes

(1) Ziegler, T. *Chem. Rev.* **1991**, *91*, 651.
(2) St. Amant, A.; Cornell, W. D.; Kollmann, P. A.; Halgren, T. A. *J. Comput. Chem.* **1995**, *16*, 1483.
(3) Becke, A. D. *Phys. Rev. A* **1988**, *38*, 3098.
(4) Lee, C.; Yang, W.; Parr, R. G. *Phys. Rev. B* **1988**, *37*, 785.
(5) Johnson, B. G.; Gill, P. M. W.; Pople, J. A. *J. Chem. Phys.* **1993**, *98*, 5612.
(6) Becke, A. D. *J. Chem. Phys.* **1993**, *98*, 5648.
(7) Frisch, M. J.; Trucks, G. W.; Schlegel, H. B.; Gill, P. M. W.; Johnson, B. G.; Wong, M. W.; Foresman, J. B.; Robb, M. A.; Head-Gordon, M.; Replogle, E. S.; Gomperts, R.; Andres, J. L.; Raghavachari, K.; Binkley, J. S.; Gonzalez, C.; Martin, R. L.; Fox, D. J.; Defrees, D. J.; Baker, J.; Stewart, J. J. P.; Pople, J. A. *Gaussian 92/DFT*; Gaussian, Inc.: Pittsburgh, PA, 1993.
(8) Frisch, M. J.; Trucks, G. W.; Schlegel, H. B.; Gill, P. M. W.; Johnson, B. G.; Robb, M. A.; Cheeseman, J. R.; Keith, T.; Petersson, G. A.; Montgomery, J. A.; Raghavachari, K.; Al-Laham, M. A.; Zakrzewski, V. G.; Ortiz, J. V.; Foresman, J. B.; Cioslowski, J.; Stefanov, B. B.; Nanayakkara, A.; Challacombe, M.; Peng, C. Y.; Ayala, P. Y.; Chen, W.; Wong, M. W.; Andres, J. L.; Replogle, E. S.; Gomperts, R.; Martin, R. L.; Fox, D. J.; Binkley, J. S.; Defrees, D. J.; Baker, J.; Stewart, J. J. P.; Head-Gordon, M.; Gonzalez, C.; Pople, J. A. *Gaussian 94*; Gaussian, Inc.: Pittsburgh, PA, 1995.
(9) Rauhut, G.; Pulay, P. *J. Phys. Chem.* **1995**, *99*, 3093.
(10) Eriksson, L. A.; Lunell, S.; Boyd, R. J. *J. Am. Chem. Soc.* **1993**, *115*, 6896.
(11) Hutter, M.; Clark, T. *J. Am. Chem. Soc.* **1996**, *118*, 7574.
(12) Ghosh, A. *J. Am. Chem. Soc.* **1995**, *117*, 4691.
(13) Wheeler, R. A. *J. Am. Chem. Soc.* **1994**, *116*, 11048.
(14) Boesch, S. E.; Grafton, A. K.; Wheeler, R. A. *J. Phys. Chem.* **1996**, *100*, 10083.
(15) Qin, Y.; Wheeler, R. A. *J. Chem. Phys.* **1995**, *102*, 1689.
(16) Brouwer, A. M.; Wilbrandt, R. *J. Phys. Chem.* **1996**, *100*, 9678.
(17) Chipman, D. M.; Liu, R.; Zhou, X.; Pulay, P. *J. Chem. Phys.* **1994**, *100*, 5023.
(18) Langkilde, F. W.; Bajdor, K.; Wilbrandt, R.; Negri, F.; Zerbetto; F. Orlandi, G. *J. Chem. Phys.* **1994**, *100*, 3503.
(19) Brouwer, A. M.; Langkilde, F. W.; Bajdor, K.; Wilbrandt, R. *Chem. Phys. Lett.* **1994**, *225*, 386.
(20) Poizat, O.; Bourkba, A.; Buntinx, G.; Deffontaine, A.; Bridoux, M. *J. Chem. Phys.* **1987**, *87*, 6379.
(21) de Boer, J. L.; Vos, A. *Acta Crystallogr.* **1972**, *B28*, 835.
(22) Brouwer, A. M.; Wiering, P. G.; Zwier, J. M.; Langkilde, F. W.; Wilbrandt, R. *Acta Chem. Scand.* **1997**, *51*, 217.
(23) Scott, A. P.; Radom, L. *J. Phys. Chem.* **1996**, *100*, 16502.
(24) El-Azhary, A. A.; Suter, H. U. *J. Phys. Chem.* **1996**, *100*, 15056.
(25) de Boer, J. L.; Vos, A. *Acta Crystallogr.* **1972**, *B28*, 839.
(26) Song, X.; Yang, M.; Davidson, E. R.; Reilly, J. P. *J. Chem. Phys.* **1993**, *99*, 3224.
(27) Marcus, R. A.; Sutin, N. *Biochim. Biophys. Acta* **1985**, *811*, 265.
(28) Grampp, G.; Jaenicke, W. *Ber. Bunsen-ges. Phys. Chem.* **1991**, *95*, 904.
(29) Nelsen, S. F.; Yunta, M. J. R. *J. Phys. Org. Chem.* **1994**, *7*, 55.
(30) Rauhut, G.; Clark, T. *J. Am. Chem. Soc.* **1993**, *115*, 9127.
(31) Nelsen, S. F. *Adv. Electron Transfer Chem.* **1993**, *3*, 168.
(32) Grampp, G.; Jaenicke, W. *Ber. Bunsen-Ges. Phys. Chem.* **1984**, *88*, 325.
(33) Marcus, R. A. *J. Chem. Phys.* **1956**, *24*, 966.
(34) Klimkans, A.; Larsson, S. *Chem. Phys.* **1994**, *189*, 25.
(35) Jakobsen, S.; Mikkelsen, K. V.; Pedersen, S. U. *J. Phys. Chem.* **1996**, *100*, 7411.
(36) Ernstbrunner, E. E.; Girling, R. B.; Grossman, W. E. L.; Hester, R. E. *J. Chem. Soc., Faraday Trans. 2* **1978**, 501.
(37) Forster, M.; Hester, R. E. *J. Chem. Soc., Faraday Trans. 2* **1981**, *77*, 1535.
(38) Hester, R. E.; Williams, K. P. J. *J. Chem. Soc., Perkin Trans. 2* **1982**, 559.
(39) Chipman, D. M.; Sun, Q.; Tripathi, G. N. R. *J. Chem. Phys.* **1992**, *97*, 8073.
(40) Brouwer, A. M.; Zwier, J. M.; Bajdor, K.; Langkilde, F. W.; Wilbrandt, R. To be published.

(41) Bally, T. Electronic Structure, Spectroscopy, and Photochemistry of Organic Radical Cations. In *Radical Ionic Systems*; Lund, A., Shiotani, M., Eds.; Kluwer: dordrecht, 1991; p 3.

(42) Hiberty, P. C.; Humbel, S.; Danovich, D.; Shaik, S. *J. Am. Chem. Soc.* **1995**, *117*, 9003.

(43) Davidson, E. R.; Borden, W. T. *J. Phys. Chem.* **1983**, *87*, 4783.

(44) Brouwer, A. M.; Krijnen, B. *J. Org. Chem.* **1995**, *60*, 32.

(45) Hoffmann, R. *Acc. Chem. Res.* **1971**, *4*, 1.

(46) Gleiter, R.; Stohrer, W.-D.; Hoffmann, R. *Helv. Chim. Acta* **1972**, *55*, 893.

(47) Poizat, O.; Guichard, V.; Buntinx, G. *J. Chem. Phys.* **1989**, *90*, 4697.

(48) Foresman, J. B.; Keith, T. A.; Wiberg, K. B.; Snoonia, J.; Frisch, M. J. *J. Phys. Chem.* **1996**, *100*, 16098.

(49) Lindsay Smith, J. R.; Masheder, D. *J. Chem. Soc., Perkin Trans. 2* **1977**, 1732.

(50) Brouwer, A. M.; Mout, R. D.; Maassen van den Brink, P. H.; van Ramesdonk, H. J.; Verhoeven, J. W.; Warman, J. M.; Jonker, S. A. *Chem. Phys. Lett.* **1991**, *180*, 556.

(51) Lauteslager, X. Y.; Wegewijs, B.; Verhoeven, J. W.; Brouwer, A. M. *J. Photochem. Photobiol. A* **1996**, *98*, 121.

(52) von der Haar, T.; Hebecker, A.; Il'ichev, Y.; Jiang, Y.; Kühnle, W.; Zachariasse, K. *Recl. Trav. Chim. Pays-Bas* **1995**, *114*, 430.

(53) Schneider, S.; Geiselhart, P.; Seel, G.; Lewis, F. D.; Dykstra, R. E.; Nepras, M. J. *J. Phys. Chem.* **1989**, *93*, 3112.

(54) Ikemoto, I.; Katagiri, G.; Nishimura, S.; Yakushi, K.; Kuroda, H. *Acta Crystallogr.* **1979**, *B35*, 2264.

(55) Allen, F. H.; Kennard, O. *Chem. Des. Autom. News* **1993**, *8*, 31.

(56) Ohashi, Y.; Iwasaki, H.; Saito, Y. *Bull. Chem. Soc. Jpn.* **1967**, *40*, 1789.

(57) Murov, S. L.; Carmichael, I.; Hug, G. L. *Handbook of Photochemistry*, 2nd ed.; Marcel Dekker: New York, 1993.

(58) Nelsen, S. F.; Buschek, J. M. *J. Am. Chem. Soc.* **1974**, *96*, 7930.

(59) Halpern, A. M.; Gartman, T. *J. Am. Chem. Soc.* **1974**, *96*, 1393.

(60) Rozeboom, M. D.; Houk, K. N. *J. Am. Chem. Soc.* **1982**, *104*, 1189.